Mitochondrial effects on fertility and longevity in *Tigriopus californicus* contradict predictions of the mother's curse hypothesis

SUMMARY

Strict maternal inheritance of mitochondria favors the evolutionary accumulation of sex-biased fitness effects, as mitochondrial evolution occurs exclusively in female lineages. The "mother's curse" hypothesis proposes that male-harming mutations should accumulate in mitochondrial genomes when they have neutral or beneficial effects on female fitness. Rigorous empirical tests have largely focused on *Drosophila*, where support for the predictions of mother's curse has been mixed. We investigated the impact of mother's curse mutations in *Tigriopus californicus,* a minute crustacean. Using nonrecombinant backcrosses, we introgressed four divergent mitochondrial haplotypes into two nuclear backgrounds and recorded measures of fertility and longevity. We found that the phenotypic effects of mitochondrial mutations were context-dependent, being influenced by the nuclear-background in which they were expressed, as well as the sex of the individual and rearing temperature. Mitochondrial haplotype effects were greater for fertility than longevity, and temperature effects were greater for longevity. However, in opposition to mother's curse expectations, females had a higher level of mitochondrial genetic variance than males for both fertility and longevity, and there was no evidence for mitochondrial mutations favoring female performance at the cost of male performance. Together, this indicates that selection on mitochondrial variation has not resulted in the accumulation of male mutation load in *Tigriopus californicus*.

22

23 # Introduction

24 In eukaryotes, life is powered by mitochondria - cytoplasmic organelles capable of producing
25 energy in the form of ATP. Originating from an ancient symbiosis over 2 billion years ago,
26 mitochondria provided the energy required for the evolution and diversification of multicellular
27 organisms[1–3]. Over evolutionary history, mitochondrial genomes have retained their ancestral
28 genetic codes and a few dozen genes while dramatically reducing their genome size through
29 deletion and gene transfer to the nucleus. Beyond the generation of ATP by oxidative
30 phosphorylation (OXPHOS), mitochondria perform additional cellular functions, including
31 initiation of apoptosis, amino acid and steroid biosynthesis, β-oxidation of fatty acids, cellular
32 signaling, and nuclear epigenetic regulation [4–8]. Nevertheless, out of 1,500 or more proteins
33 found in the mitochondrion, only the 13 membrane-bound ETC complexes are encoded by the
34 mitochondrial genome, with the rest being encoded by nuclear DNA[9,10]. The coevolution of
35 mitochondrial and nuclear genomes is thus an ancient yet ongoing process, involving the
36 evolutionary fine-tuning of various molecular interactions (i.e. protein-protein, protein-DNA,
37 and protein-RNA) required for the accurate replication and transcription of mtDNA, translation
38 of mtDNA-encoded proteins, and efficient cellular respiration. Mutation rates are generally
39 higher in mtDNA than in nDNA[11,12] leading to a continuous introduction of new mitochondrial
40 alleles. With asexual transmission and lack of recombination in mitochondria, novel alleles are
41 likely to persist, even when slightly deleterious, due to the potential masking effect of linkage
42 disequilibrium on mitochondrial genetic variation and reduced efficacy of natural selection[13].
43 Nevertheless, mtDNA likely experiences recurrent adaptive evolution via selective sweeps acting
44 on traits such as respiratory efficiency and mitonuclear coadaptation[14–18]. In natural populations,

45 mitochondrial fitness variation is likely to be present at substantial levels and may make a
46 meaningful contribution to adaptation and diversification[19]. The distribution of fitness effects
47 among mtDNA mutations is also likely to differ between the sexes, owing to the maternal
48 inheritance of mitochondria[20–22]. Strict maternal inheritance favors the evolutionary
49 accumulation of sex-biased fitness effects, as it is expected to preclude any opportunity for
50 evolution in males, forming a sex-specific selective sieve.

51 Under maternal inheritance, mitochondrial evolution is thought to be restricted to female
52 lineages, leading to the accumulation of male-harming mutations when they have neutral or
53 beneficial effects on female fitness (i.e. "mother's curse"[21,23]). Initial evidence for the mother's
54 curse hypothesis (MCH) centered on evidence that sperm motility in humans and other taxa was
55 linked to mitochondrial function[24,25,23] therefore sperm are more exposed to deleterious effects
56 of mtDNA mutations than ova. The MCH has also been proposed to impact viability, and even to
57 contribute to the taxonomically widespread pattern of shorter male lifespans[26]. Theoretical work,
58 however, shows that conditions favoring the spread of mother's curse mutations can be limited
59 by even modest levels of inbreeding and kin selection, allowing for an adaptive response to
60 mtDNA alleles impacting male viability and fertility[27–29]. Nevertheless, interest in MCH has
61 increased steadily in recent years leading to formal tests of the hypothesis, mostly in *Drosophila*,
62 utilizing carefully constructed mitochondrial-nuclear (mitonuclear) hybrids with divergent
63 mtDNA haplotypes backcrossed into an isogenic nuclear background. The most direct test of
64 MCH focuses on the effects of mutational variation in mtDNA, which are predicted to confer
65 larger trait variance in males. A second major prediction focuses on the subset of alleles that are
66 directly sexually antagonistic, which could lead to a negative intersexual genetic correlation
67 across haplotypes. A third prediction is that experimental disruption of mitonuclear coadaptation

68 will be more detrimental to males than females. Studies using the mitonuclear hybrid approach
69 have shown both support[26,30–34], and rejection[35–38] of the mother's curse hypothesis.
70 Understanding the pervasiveness of mother's curse is crucial given its fundamental
71 implications for the evolution of sexual dimorphism, as well as very practical consequences for
72 conservation breeding programs and medicine (particularly mitochondrial replacement theory
73 and male-biased mitochondrial disease). While past work has focused on *Drosophila*, the
74 predominance of maternal inheritance of mitochondria in eukaryotes allows for a taxonomically
75 diverse investigation of the generality of mother's curse. Here we test predictions of the MCH
76 using the splash-pool copepod *Tigriopus californicus*, an arthropod that shares a common
77 ancestor with *Drosophila* at least 450 million years ago. We used a genetic panel of mitonuclear
78 hybrids to assay both fertility and longevity. As fertility genes are likely sex-specific and
79 viability genes are likely shared between the sexes (see review[39]), we predict that mitonuclear
80 mismatch will lead to stronger sex bias for fertility than longevity. Additionally, we measured
81 the impact of high environmental temperature on these traits, as mild mitonuclear mismatch can
82 be expected to be unmasked under higher metabolic demand[40]. Populations of *T. californicus*
83 show extreme genetic divergence over short geographical distances[41–43] while remaining
84 somewhat tolerant of hybridization, producing viable and fertile offspring[44,45]. Nucleotide
85 divergence in *T. californicus* extends across the mtDNA genome, involving coding and
86 noncoding genes, and can exceed 20% between distant populations. *T. californicus* also differ
87 from most model organisms in that they lack heteromorphic chromosomes - sex is determined by
88 the inheritance of multiple, unlinked genes in combination with environmental effects (polygenic
89 sex determination)[46–48]. While rarely utilized in evolutionary biology, polygenic sex
90 determination provides an advantage for testing sex-specific mitochondrial effects as sex

differences cannot be attributed to the effects of sex chromosomes. Importantly, despite the lack of heteromorphic sex chromosomes, there is marked sexual dimorphism in *T. californicus* and considerable evidence for sex-specific effects in multiple traits (thermal tolerance[49,50]; salinity tolerance[51,52]; resistance to toxins[52]; intrinsic hybridization stress[47]) in which males are generally the weaker sex.

Methods

Population sampling

Populations of *T. californicus* are distributed in supralittoral "splash pools" along the Pacific coast of North America. Copepods were originally collected from supralittoral pools at four locations (Figure 1A): Friday Harbor, WA (FHL: 48.55 N,123.01 W), La Jolla, CA (LJ: 32.83 N,117.27 W), Bird Rock, CA (BR: 32.82 N,117.27 W), and San Diego, CA (SD: 32.7460 N,117.2551 W). Isofemale lines were initiated from a single female fertilized by a single male, and maintained at 20°C on a 12h:12h light:dark cycle in standard culture media (three times filtered seawater from Wrigley Marine Science Center, Santa Catalina Island, CA; 0.1g/l of Spirulina (BRAND) and 0.1g/l ground Tetramin (Tetra®) Tropical fish food flakes). All lines were maintained in petri dishes for ≥ 5 years under these conditions and periodically fed additional Spirulina and ground Tetramin® tropical fish food and rehydrated with DI water whenever necessary to maintain approximately 35 ppt salinity. Prior to experimentation, we sequenced samples from each isofemale line at the 12S ribosomal RNA locus (Forward primer: CCAAGATACTTTAGGGATAACAGC; Reverse primer: CTGTTCTATCAAAACAGCCCT; fragment size: 687 base pairs) to rule out cross-contamination.

114 **Mitonuclear hybrid panel**

115 In *Tigriopus*, meiosis is chiasmatic in males but achiasmatic in females, yielding recombinant
116 sperm and non-recombinant ova. This allows us to backcross mitochondria from the population
117 of the dam into that of the sire while preventing nuclear recombination between populations.
118 Because sexes in *T. californicus* are not easily distinguished before maturity, we allowed males
119 to clasp female siblings with their geniculate first antennae in order to ensure the sex of females.
120 We moved clasped pairs onto filter paper and quickly separated them using entomological pins
121 under a microscope. We backcrossed FHL, BR, LJ, and SD dams to SD and BR sires for 10
122 generations (Figure 1B), resulting in an average proportion of $1 - \frac{1}{2}^{(b+1)}$ (where b is equal to the
123 number of backcross generations) or 99.95% of the sire's nuclear genome, assuming no
124 selection. For each cross, we established 4 replicates, each maintained in 12-well plates
125 containing standard culture media. All crosses were fed weekly with additional Spirulina and
126 ground Tetramin® fish food and rehydrated with DI water whenever necessary to maintain
127 approximately 35 ppt salinity.

128

129 **Trait measurement and modeling**

130 For each of our mitonuclear hybrid lines, we measured three fitness components (fertility,
131 lifespan, and age-specific rate of survival) for males and females reared at two contrasting
132 temperature regimes (15ºC and 25ºC). In order to achieve an adequate sample size for each
133 mtDNA haplotype and sex, it was necessary to set up multiple families from each mitonuclear
134 hybrid line. Each family was composed of up to four clutches of fertilized eggs derived from a
135 single mitonuclear hybrid or control female (dam). Dams were maintained at standard conditions
136 and checked daily for the presence of hatched eggsacs. For each dam, we alternated moving up

137 to four hatched eggsacs to 15ºC and 25ºC (Figure 1B) so that clutch order was orthogonal to
138 temperature in both fertility and longevity experiments. Individuals were maintained at the same
139 temperature for the duration of the fertility or longevity experiment.
140
141 **Longevity**
142 Individual animals were separated into wells in a 24-well plate once they developed to the
143 juvenile copepodid stage and were checked three times a week. The first measurement we
144 recorded was the sex-specific age of reproductive maturity. For males, this occurred with the
145 development of geniculate first antennae (claspers) and for females with the development of
146 eggs, which can be seen through the translucent body. We continued monitoring longevity
147 experiments three times a week, recording the age of death of individuals until all had expired.
148
149 We performed linear mixed-effects modeling on family sex ratio using sex information
150 from our longevity experiment, comparing mtDNA x nDNA interactions with the impact of
151 mitonuclear status on family sex ratio. We also conducted a separate experiment, using different
152 families, measuring mortality occurring before sexual maturity (Document S1, Figure S1). We
153 were able to measure the age at the naupliar-copepodid transition, duration of the copepodid
154 stage, and the sex-specific age of reproductive maturity, and perform linear mixed-effects
155 modeling investigating the influence of genetic (mtDNA, nDNA) and environmental
156 (temperature) influence on these larval life-history parameters.
157

158 **Sex-specific fertility**

159 For female fertility experiments, all individuals from hatched eggsacs were separated into
160 individual wells in a 24-well plate once they developed to the juvenile copepodid stage. To each
161 well, we added a single wild-caught adult male from the appropriate locality (SD or BR),
162 matching the paternal line of the individual. Males were added to every well because sexes are
163 difficult to distinguish morphologically in immature *T. californicus* and we wanted to ensure that
164 each female was paired with an adult male before sexual maturity. Mate clasping typically occurs
165 between adult males and juvenile females, and rarely occurs with mature females once they
166 begin extruding non-fertilized eggsacs. We also ran experiments utilizing sib-pairs in parallel to
167 compare the impact of mating with mitonuclear hybrid males versus wild-type males on female
168 fertility (Document S1). Plates were maintained at the appropriate temperature (15ºC or 25ºC)
169 and checked three times a week until females produced an eggsac. As we utilized several
170 hundred plates in our experiment, it became necessary to maximize incubator space. Therefore,
171 we placed gravid females from the same family and clutch together in petri dishes until they
172 reached experimental age. Because individuals develop twice as fast at 25ºC as at 15ºC, we used
173 temperature-specific ages for our experiment in order to minimize age-related variation. Once
174 individuals reared at 25°C reached 35 days of age, and individuals reared at 15°C reached 70
175 days of age, we moved them into separate dishes and maintained them at the correct temperature,
176 checking them three times a week until eggsacs hatched. Upon hatching, each individual larval
177 nauplius was counted under a dissecting microscope to measure female hatching number.

178 For male fertility experiments, we removed males from each of the four clutches in a
179 family and allowed them to age for the appropriate temperature (35 days old for 25ºC and 70
180 days old for 15ºC). Once at the appropriate age, each male was pipetted into a petri dish with six

181 wild-caught juvenile females from the appropriate locality (BR or SD) to match the paternal
182 nuclear line. To ensure that wild-caught juveniles were female, we selected clasped pairs from
183 culture within 0-2 weeks of collection and separated pairs under a dissecting microscope. Care
184 was taken to provide males with females of consistent and reasonably large size, to reduce
185 variation across experiments. Each experimental male and six wild-caught females were allowed
186 14 days to mate in a petri dish at the appropriate temperature. After 14 days, females were
187 isolated into a 6-well plate and scored for the presence or absence of any offspring indicating a
188 successful mating. We recorded male remating success as the ratio of successful matings to the
189 number of surviving females.
190

191 **Parametric and nonparametric trait modeling**

192 For our trait modeling, we performed three types of linear models: sex-effect modeling,
193 coevolutionary status modeling, and best-fit models. Sex-effect models measure sex effects
194 impacted by mtDNA and nDNA variation and their interactions. If mother's curse mutations are
195 present, they may exist in additive (Sex x mtDNA) or epistatic (Sex x mtDNA x nDNA) form.
196 Sex differences may also be encoded by nuclear genes, described by the (Sex x nDNA) term. In
197 order to compare fertility experiments across the two sexes, individual measurements of fertility
198 were normalized to the mean of the appropriate matched control line reared at the same
199 temperature (e.x. male *i* from FHLxSD at 15°C / mean of all males from SDxSD at 15°C). We
200 performed model testing on the four sex-effect models using the *model.sel* function in the
201 MuMIn[53] R package, which ranks models based on their AIC_C values. Model contrasts for sex
202 differences were performed using the *pairs* function from the emmeans[54] R package .
203 Coevolutionary status models measure the impact of disrupting coevolved mitonuclear

204 combinations on sex-specific data grouped by temperature and nDNA. These models included
205 coevolutionary status as a fixed-effect term. Modeling for best-fit utilized an "all-subset"
206 approach, where all possible combinations of predictors were compared using the *MuMIn*
207 function *dredge*. Models with the highest weight and lowest AIC_C were designated as best-fit.
208 Both fertility and longevity models included temperature, nDNA, mtDNA and all possible
209 interactions as fixed-effects terms in initial models and were performed separately for each sex.
210 For fertility, we used raw sex-specific fertility (males: remating success, females: hatching
211 number). All linear mixed-effects modeling was performed using the *lmer* function from the
212 lme4[55] R package and included clutch nested within family as a random-effect term. We used
213 type III ANOVA to estimate significance for model main effects and interaction terms using the
214 *Anova* function from the car[56] R package.
215 We performed parametric regression of survivorship for each nuclear, temperature, and
216 sex combination against the Gompertz distribution [57], estimating the shape (α) and rate (β)
217 parameters using the R package flexsurv[58]. Parameters were estimated by maximum likelihood,
218 with those defined to be positive estimated on a log scale. Confidence intervals were estimated
219 from the Hessian at maximum, and then transformed back to the original scale (days). The shape
220 of the resulting distributions, ln(α), describe the initial mortality rate or frailty of the samples,
221 while the rate (β) parameter describes the age-independent rate of mortality acceleration or rate
222 of senescence. We employed Kruskal-Wallis one-way analysis of variance to estimate the
223 significance of parameter estimates produced by parametric survival models using the
224 *kruskal.test* function from the stats[59] R package.
225

226 **Mitochondrial coefficient of variation**

227 One prediction of the mother's curse hypothesis is that the accumulation of male-affecting
228 variation should lead to a higher mitochondrial coefficient of variation (CV_{mt}) in males than in
229 females. Using the *boot*[60,61] package in R, bootstrapped CV_{mt} was computed by resampling raw
230 trait means for each mitochondrial line using 1000 replicates with replacement and calculating
231 the coefficient of variation among mitochondrial lines ($CV = \sigma/\mu$) for each nuclear, sex, and
232 temperature combination. Hypothesis testing was performed to compare male and female CV_{mt}
233 using a sign test as implemented in the *SIGN.test* function in the BSDA[62] R package.

234

235 **Genetic correlation among haplotypes**

236 Mother's curse mutations are likely to reach fixation fastest when they confer a fitness advantage
237 to females, resulting in sexual conflict when they simultaneously result in low fitness in males.
238 When enough mtDNA variation is involved in sexual conflict, a negative intersexual correlation
239 may be observed across haplotypes for a given trait. We measured the correlation between
240 haplotype means for fertility and median longevity, comparing traits within sexes (intrasexual
241 correlation) and also comparing the sexes for a given trait (intersexual correlation). We used
242 bootstrapped estimates of Pearson's coefficient using the boot R package along with the *cor*
243 function from the stats R package, recording 1000 samples for each comparison. Equi-tailed,
244 two-sided nonparametric confidence intervals were generated from the first order normal
245 approximation with a confidence level of 0.95 using the *boot.ci* function from the boot package
246 in R.

247

248 **Whole genome sequencing**

249 For each isofemale and mitonuclear hybrid line, we extracted DNA from 10 males and 10
250 females using Zymo quick-DNA preps and quantified DNA yields using Qubit HS dsDNA
251 quantification kits. Because female *T. californicus* yield approximately 2.12x more DNA than
252 males, we pooled 2 ng of DNA from each of the 20 individuals per line for library preparation.
253 DNA pools were sheared using a Covaris S2 sonicator with microTUBE-50 AFA tubes, and
254 sequencing libraries were prepared using Qiagen QIAseq Ultralow Input kits following
255 instructions. Mitonuclear hybrid libraries were pooled together in equimolar amounts and
256 sequenced together on a single lane of Illumina HiSeq4000 (PE-150), and the parental isofemale
257 libraries were pooled and sequenced on a separate lane. Sequence reads were quality trimmed
258 using trimmomatic[63] v0.36, and paired reads were filtered for mitochondrial reads using the
259 filter_reads.pl perl script included with the NOVOPlasty[64] software. We assembled consensus
260 mtDNA genomes from each sequenced isofemale line, by utilizing the appropriate mtDNA
261 reference from a previous publication which included the SD, BR, and FHL populations[18]. A
262 reference mtDNA genome did not exist for the LJ population, so those reads were mapped to the
263 BR mtDNA reference. We annotated our *de novo* assembled genomes using the Mitos[65] 2.0
264 software, each containing all 13 protein coding genes, and the majority of non-coding RNAs.
265 Following this, we mapped all trimmed and paired reads to the *T. californicus* reference genome
266 assembly (NCBI accession: GCA_007210705.1) along with the appropriate mitochondrial
267 genome using stampy[66] v1.0.32 (substitutionrate=0.05). Following the removal of PCR and
268 optical duplicates using picard[67] MarkDuplicates, we called variants for each sequenced pool
269 using samtools[68] mpileup.

270 We estimated pairwise nuclear divergence for isofemale lines in a sliding window
271 approach. For each comparison, we calculated F_{ST} using a sliding window of 10,000 bp,
272 requiring a depth of 40x coverage, and minimum PHRED base quality score of 30 using the fst-
273 sliding.pl perl script included with popoolation v1.2.2. For parental mitochondrial divergence,
274 we aligned whole mtDNA genomes using progressiveMauve[69] along with mtDNA genome
275 sequences from an outgroup population from San Roque, Baja California Sur, Mexico to produce
276 rooted trees, and measured divergence (d_{XY}) using the calculate-dxy.pl perl script included with
277 popoolation v1.2.2. We also measured divergence at synonymous and nonsynonymous sites by
278 aligning protein-coding sequences with MACSE [70] v2, constructing neighbor joining trees with
279 ClustalW [71] and analyzing these data with codeml from the PAML suite [72] using the null model
280 (M0), assuming a uniform selective pressure among sites.
281

282 **Confirming mitonuclear genetic status of hybrids**

283 To test for potential selection or accidental introgression, we measured allele frequencies at a set
284 of divergent sites for each paternal line's nuclear genome. A Fisher's exact test for significant
285 allele frequency differences for nDNA from the maternal and paternal lines was conducted using
286 popoolation[73] v1.201, requiring a minimum depth of 20x coverage. In mitonuclear hybrids, sites
287 with no significant differences (alpha > 0.05) to the paternal line were considered "paternally
288 concordant" and significantly different sites (alpha <= 0.05) were considered "paternally
289 discordant". Because significance may be determined by variations in the same alleles between
290 lines, we recorded paternally discordant sites with alleles matching maternal lines as "maternally
291 concordant" when they were absent in the paternal nDNA. Paternal concordance rates were
292 recorded by measuring the proportion of sites that were not maternally concordant to the total

293 number of sites. We also examined mitonuclear hybrid lines for the presence of paternally
294 inherited mtDNA. This was accomplished by mapping trimmed and paired sequence reads to the
295 reference genome as well as all mtDNA haplotypes simultaneously. We measured depth of
296 coverage using samtools depth command to identify any potential sources of contamination.
297
298

299 Results

300 DNA sequencing

301 Illumina HiSeq 4000 sequencing yielded an average of 34.7 million reads for mitonuclear hybrid
302 line pools, and 76.1 million reads for inbred line pools. Following quality trimming and mapping
303 of paired reads to the appropriate references, an average of 29 million reads mapped for cybrid
304 pools, and 61 million reads mapped for maternal and paternal line pools. Average nuclear
305 genome coverage across inbred lines was 91.88% at a mean depth of coverage of 26x. Across
306 the mitochondrial genome, the mean depth of coverage was 2670X, and genome coverage was
307 100%. Nuclear divergence (F_{ST}) between paternal lines ranged from 0.049 to 0.369 in lines with
308 BR nDNA, and from 0.102 to 0.378 in lines with SD nDNA (Figure 1C). Mitochondrial
309 divergence (d_{XY}) between parental lines ranged from 0.7% to 21.1% in BR nDNA lines, and
310 9.6% to 20.6% in SD nDNA lines. The mitonuclear hybrid panel represented a wide range of
311 mitochondrial variation, with as few as 13 amino acid substitutions between the BR and LJ
312 mitotypes, 170 aa substitutions between the BR and SD nuclear line mitotypes, and 555 aa
313 substitutions between SD and FHL haplotypes. The highly divergent FHL haplotype also
314 differed from the BR & LJ haplotypes by 546 aa substitutions.

315 For each mitonuclear hybrid line, we measured allele frequencies at an average of 580k
316 divergent nDNA SNPs between parental lines. We found that alleles were mostly concordant
317 with paternal nDNA, with limited evidence of introgression from maternal nDNA, with paternal
318 concordance rates ranging from 99.15% - 100% (Figure 1C). To test for potential mtDNA
319 contamination via paternal leakage or experimental error, we compared depth of coverage across
320 all mtDNA haplotypes, since mtDNA positions and alleles are not comparable across haplotypes.
321 We found that the percent maternally matching depth ranged from 94.09% to 99.81%, while the
322 percent of paternally matching depth ranged from 0.02% to 0.28% providing limited evidence
323 for contaminating mtDNA (Figure 1C).
324
325 **Trait measurements and modeling**
326 Despite initially setting up four replicates for each mitonuclear hybrid line, low productivity led
327 to extinction of several replicates, forcing us to proceed with one replicate per line to keep our
328 experiment balanced. We measured the hatching number for 182 females coming from 41
329 families reared at 15ºC and 216 females from 40 families reared at 25ºC. Male remating success
330 was measured for 491 males, using a total of 2,458 wild-caught females. Since 378 females died
331 over the course of the experiment, we discarded 31 males that had fewer than four out of six
332 females remaining in order to reduce variation associated with differential access to females.
333 Therefore, our male remating experiment is based on 235 males from 68 families reared at 15ºC
334 and 225 males from 76 families reared at 25ºC. The average male successfully copulated with
335 2.45 females in the span of 14 days when reared at 15°C, declining to 2.04 females at 25°C
336 representing a 17% reduction. In the average female clutch, 30.05 eggs hatched at 15°C,
337 declining to 21.50 eggs hatching at 25°C representing a 28% reduction. Female hatching number

338 declined an average of 31.16% in mitonuclear hybrid lines when females were bred with siblings
339 as opposed to wild-caught males (Document S1, Figure S2. Lifespan, frailty, and rate of
340 senescence was measured for 3,072 individuals, with 1,531 individuals from 89 families reared
341 at 15ºC, and 1,541 individuals from 77 families reared at 25ºC.
342
343 Experiments on early developmental stages indicate that mortality rate occurring before sexual
344 maturity was very high, ranging from 14.6% to 90.6% mortality depending on cross and
345 temperature (Document S1, Figure S1. Naupliar stages had the highest mortality, ranging from
346 4.2% to 84.4%, while copepodid stages ranged from 1.5% to 27.9% mortality. Linear mixed-
347 effects modeling showed that measurements describing the development rate varied significantly
348 with mtDNA x nDNA interactions and rearing temperature, with rates increasing at higher
349 temperature.
350
351 **Sex-effect modeling**
352 Model contrasts revealed mostly male-biased values for longevity (longer lifespan), and mixed
353 bias for fertility with three out of six significant contrasts being female biased (Figure 2A).
354 Model selection comparing the four sex-effects models (Table S1) revealed that models
355 including three-way sex x nDNA x mtDNA interaction term fit the trait data best in all
356 temperature and trait combinations except for relative fertility at 15°C, which was better fit with
357 sex x nDNA interactions (ΔAIC = 17.35). None of the sex-effects models uncovered significant
358 sex x mtDNA interactions (Table S2). However, we do see that sex x nDNA and sex x mtDNA x
359 nDNA interactions are a significant influence on fertility variation (Figure 2B).
360

361 **Mitonuclear coevolutionary status modeling**

362 We found that neither fertility nor longevity were influenced by mitonuclear status (matched vs.
363 mismatched), as indicated from type III ANOVA on fitted parameters (Table S3). Family sex
364 ratio was significantly influenced by mitonuclear status (χ^2= 18.51, p = 1.7e-5), as indicated in
365 linear mixed-effects modeling (Document S1, Figure S3), as well as nDNA x mitonuclear status
366 interactions (χ^2= 28.77, p = 8.1e-8). Results using mortality-corrected family sex ratio data were
367 also consistent with uncorrected family sex ratio. (Table S5).

368

369 **Best-fit models**

370 Temperature significantly impacted all traits by reducing their average values (Table S4).
371 Notably, mean longevity was reduced by 102 days in 25ºC, an almost 10 day decrease per degree
372 reduction. Significant mtDNA effects were only seen in females for both hatching number (χ^2=
373 20.36, p = 1.43e-4) and longevity (χ^2= 14.66, p = 0.0021). Variation in nDNA impacted
374 longevity in both sexes (males: χ^2= 20.36, p = 6.42e-6; females: χ^2= 8.31, p = 0.0040) but
375 neither measure of fertility (female hatching number: χ^2= 1.37, p = 0.2416; male remating
376 success: χ^2= 0.15, p = 0.6991). Additionally, effects of nDNA were contingent upon rearing
377 temperature, with significant interactions between the two terms for male remating success (χ^2=
378 7.41, p = 0.0065), male longevity (χ^2= 4.19, p = 0.0407) and female longevity (χ^2= 4.05, p =
379 0.0442). Interactions between mtDNA and nDNA were also significant for longevity in females
380 (χ^2= 12.03, p = 0.0073) and in a three-way interaction with temperature for male remating
381 success (χ^2= 16.95, p = 7.22e-4). Mitochondrial effects impacted fertility more than longevity
382 (Figure 2C, p = 3.2e-4), while nuclear effects impacted both traits equally (p = 0.95) and
383 temperature affected longevity more than fertility (p = 1.5e-6). Linear mixed-effects modeling of

384 family sex ratio indicated significant influence of temperature ($\chi^2 = 10.02$, $p = 0.0015$), mtDNA
385 haplotype ($\chi^2 = 28.35$, $p = 3.1e-6$), as well as interactions between mtDNA and nDNA ($\chi^2 =$
386 31.98, $p = 1.6e-8$) and temperature and nDNA ($\chi^2 = 29.94$, $p = 1.4e-6$; Document S1, Figure S3).
387

388 **Parametric survivorship modeling**

389 Survivorship curves indicate a drastic reduction in longevity shifting from 15°C to 25°C, with
390 SD nDNA individuals having higher survivorship than BR nDNA individuals at 25°C (Figure
391 3A). Additionally, we see that median longevity is sex-biased in SD nDNA individuals reared at
392 15°C, with higher male longevity (Figure 3A insert, Wilcoxon rank sum test, p = 0.004). Rearing
393 temperature affected both frailty ($\chi^2 = 22.55$, $p = 2.05e-6$) and rate of senescence ($\chi^2 = 23.27$, $p =$
394 $1.41e-6$) in a similar manner, with the higher temperature leading to increased frailty and
395 increased rate of senescence (Table S6). Mitochondrial haplotype showed no significant
396 contribution to Gompertz parameters when reared at either 15ºC or 25ºC (Table S6). We found
397 significant sexual dimorphism in frailty and senescence in individuals reared at 25ºC, but not
398 those reared at 15ºC (Figure 3B). When reared at 25ºC, females had lower frailty than males, but
399 a higher rate of senescence and while this pattern held in both nDNA backgrounds, it was
400 nonsignificant in BR nDNA lines (Table S6).
401

402 **Mitochondrial coefficient of variation**

403 Females had significantly higher CV_{mt} than males in seven out of eight experimental groupings
404 (Figure 4A, Table S3). The median difference between male and female coefficients in these
405 groupings ranged from 0.0039 to 0.1061. In contrast, fertility in BR nDNA individuals at 25ºC

showed higher male CV_{mt} than females (median difference = -0.0993, CI = (-0.11, -0.09), $p <$ 2.2e-16).

Genetic correlation among haplotypes

Intersexual correlations for median longevity (r = 0.99; CI_{95} = 0.20, 2.00) and fertility (r = 0.84; CI_{95} = 0.08, 1.72) were significantly positive in BR nDNA individuals reared at 25ºC, while correlations for median longevity in SD nDNA individuals were also significantly positive (r = 0.85; CI_{95} = 0.04, 1.75) in individuals reared at 25ºC (Figure 4B). Intrasexual correlations between fertility and longevity were significantly positive in BR nDNA individuals of both sexes reared at 25ºC (males: r = 0.96; CI_{95} = 0.21, 1.95; females: r = 0.90; CI_{95} = 0.08, 1.86). No measures of intersexual or intrasexual correlation were significantly negative.

Discussion

Our study sought to explicitly test three predictions arising from the mother's curse hypothesis: higher mitochondrial genetic variance in males for fitness traits, negative intersexual correlation among mitochondrial haplotypes for fitness traits, and higher impact of experimental disruption of putatively coevolved mitonuclear genotypes on males. Our results did not support these predictions. Females had a higher level of mitochondrial genetic variance in seven experimental groupings and lower variance in one grouping (fertility in individuals with BR nDNA reared at 25ºC). We also found no evidence for sexual antagonism for fertility or longevity, with negative intersexual correlations found in two of eight experimental groupings (fertility in BR nDNA at 15°C and SD nDNA at 25°C) having upper confidence intervals that extended well into positive ranges (0.90 and 1.41, respectively). Overall, the intersexual

429 comparisons mimicked the intrasexual comparisons. Lastly, we did not find the significant
430 influence of coevolutionary status on fertility or longevity traits required to test the third
431 prediction.
432
433 Detecting sex-bias in mitochondrial coefficient of variation for fitness traits is arguably
434 the most direct test of the hypothesis since it emphasizes the differential accumulation of
435 mutational variation between the sexes[74]. According to the mother's curse hypothesis,
436 mitochondrial mutations causing male infertility that are neutral in females are more likely to
437 spread in a population through random drift since males are a dead-end for natural selection on
438 mtDNA. However, this argument is best applied to randomly mating populations with no
439 inbreeding. In populations with even modest levels of inbreeding, such as those with
440 geographical population structure, females will also suffer fitness insults from mother's curse
441 mutations to a certain degree since they are more likely to mate with sub-fertile siblings[27,28,75].
442 The degree to which male subfertility influences female fertility fitness can also influence these
443 dynamics. In monandrous species like *Tigriopus*, females mate only once[76,77], resulting in a
444 direct relationship between male fertility and female offspring production. In this study, we
445 showed that female hatching number dropped substantially when mated with siblings compared
446 to wild-caught males, indicating the influence of male subfertility on female fertility. However,
447 in mating systems where females mate with several males (e.g. *Drosophila*), females can be
448 safeguarded against male infertility or subfertility[78]. As a result, selection to purge male-harming
449 mtDNA mutations is expected to be strongest in species with monandry and weakest with
450 polyandry whenever inbreeding is present[75]. Studies show that *T. californicus* avoid close
451 inbreeding[79], but live in highly isolated, ephemeral populations making inbreeding all but

452 inevitable[80,81]. Additionally, while inbreeding can limit mother's curse by decreasing the
453 conditions under which male-harming alleles can spread, it can also result in the spread of
454 female-harming alleles that benefit males and lead to female-biased fitness variance [22,27]. The
455 widespread female-biased fitness variance observed in our fertility and longevity experiments
456 may therefore indicate the impact of historical inbreeding on the fixation of mitochondrial
457 divergence sampled in our study.
458
459 We predicted that sex differences due to mitochondrial haplotype effects are greater for
460 fertility than longevity, based on the expectation that fertility genes are more sex-specific than
461 viability genes[82,83]. We also predicted that the consequences of mitonuclear mismatch should
462 increase with metabolic rate associated with increased temperature. Efficient energy production
463 depends on mitochondrial function, including mitonuclear coordination. Mild mitonuclear
464 mismatches may be tolerated under low aerobic demand and yet become lethal when energetic
465 demand become higher [40,but see 82]. Increased temperature reduced measures of both fertility and
466 longevity but was more dramatic with the latter. We uncovered significant mitonuclear effects
467 impacting longevity at 25°C but not 15°C. Additionally, we found that mitonuclear x sex effects
468 were significant for fertility at 25°C, but not 15°C. Mitochondrial haplotype effects in our
469 experiment impacted fertility more than longevity, however experiments on the larval stages
470 indicate a substantial amount of mortality, influenced by temperature and mitonuclear
471 interactions, occurring before sexual maturity. Because *T. californicus* sperm are amotile,
472 declines in male fertility are not attributed to loss of sperm motility – a key marker of male
473 sterility in organisms with flagellated, motile sperm. Instead, declines in male fertility in our

474 study are likely due to the number of mature spermatids in a spermatophore, the ability of sperm
475 to maintain homeostasis while residing in the female reproductive tract, or behavior.
476 Survivorship analysis indicates that mtDNA variation had an inverse impact on frailty
477 and senescence between the sexes, similar to the 'Strehler-Mildvan (S-M) relationship[85]. When
478 reared at 25ºC, females had lower frailty than males while also having a higher rate of
479 senescence, despite having similar median longevity. One explanation for this relationship is that
480 the preferential survival of the most-frail female *T. californicus* may lead to an increase in the
481 rate of senescence for females, since frail individuals are more susceptible to aging. Male *T.*
482 *californicus* typically have lower tolerance than females to a variety of stressors, including
483 temperature, and a greater transcriptomic response to oxidative stress[49,50,52,86,87].
484
485 **Conclusion**
486 We found that the functional mtDNA effects were highly context-dependent, being
487 influenced by the nuclear-background in which they were expressed, the temperature in which
488 individuals developed, and/or the sex of the individual. We explicitly sought to test the main
489 predictions of the mother's curse hypothesis, finding patterns opposite to those predictions.
490 Support for the mother's curse hypothesis has been highly mixed to date, both theoretically and
491 empirically, with many studies rejecting these predictions. While most studies directly testing
492 predictions of the mother's curse hypothesis have used *Drosophila*, the predominance of
493 maternal inheritance of mitochondria in eukaryotes allows for a taxonomically diverse
494 investigation of the generality of mother's curse. Particularly, diversity in mating system should
495 be considered for future studies, as the fitness of females that mate with only one male will be
496 strongly determined by the fitness of her mate when there is inbreeding. Furthermore, sperm

497 diversity (motile/amotile, storage/remating) should be highlighted in order to address the
498 relevance of various mutational insults to male fitness potentially harbored by mitochondrial
499 DNA. In light of the evidence presented here and elsewhere, we suggest that accumulation of
500 male-harming mitochondrial mutations may not be a generalizable phenomenon, despite the
501 prevalence of maternal mitochondrial transmission across eukaryotes.

502
503
504
505
506
507
508
509

510 # References

511 1. Yang, D., Oyaizu, Y., Oyaizu, H., Olsen, G. J. & Woese, C. R. Mitochondrial origins. *PNAS* **82**,
512 4443–4447 (1985).
513 2. Gray, M. W., Burger, G. & Lang, B. F. Mitochondrial Evolution. *Science* **283**, 1476–1481
514 (1999).
515 3. Hedges, S. B., Blair, J. E., Venturi, M. L. & Shoe, J. L. A molecular timescale of eukaryote
516 evolution and the rise of complex multicellular life. *BMC Evol Biol* **4**, 2 (2004).
517 4. McBride, H. M., Neuspiel, M. & Wasiak, S. Mitochondria: More Than Just a Powerhouse.
518 *Current Biology* **16**, R551–R560 (2006).

519 5. Pagliarini, D. J. & Rutter, J. Hallmarks of a new era in mitochondrial biochemistry. *Genes Dev.*
520 **27**, 2615–2627 (2013).
521 6. Chandel, N. S. Mitochondria as signaling organelles. *BMC biology* **12**, 1 (2014).
522 7. Birsoy, K. *et al.* An Essential Role of the Mitochondrial Electron Transport Chain in Cell
523 Proliferation Is to Enable Aspartate Synthesis. *Cell* **162**, 540–551 (2015).
524 8. Santos, J. H. Mitochondria signaling to the epigenome: A novel role for an old organelle. *Free*
525 *Radical Biology and Medicine* **170**, 59–69 (2021).
526 9. Bar-Yaacov, D., Blumberg, A. & Mishmar, D. Mitochondrial-nuclear co-evolution and its
527 effects on OXPHOS activity and regulation. *Biochimica et Biophysica Acta (BBA) - Gene*
528 *Regulatory Mechanisms* **1819**, 1107–1111 (2012).
529 10. Lotz, C. *et al.* Characterization, design, and function of the mitochondrial proteome:
530 from organs to organisms. *J. Proteome Res.* **13**, 433–446 (2014).
531 11. Brown, W. M., George, M. & Wilson, A. C. Rapid evolution of animal mitochondrial DNA.
532 *Proc. Natl. Acad. Sci. USA* 5 (1979).
533 12. Lynch, M. Rate, molecular spectrum, and consequences of human mutation.
534 *Proceedings of the National Academy of Sciences* **107**, 961–968 (2010).
535 13. Lynch, M. & Blanchard, J. L. Deleterious mutation accumulation in organelle genomes.
536 *Genetics* **102/103**, 29–39 (1998).
537 14. Schmidt, T. R., Wu, W., Goodman, M. & Grossman, L. I. Evolution of nuclear-and
538 mitochondrial-encoded subunit interaction in cytochrome c oxidase. *Molecular Biology and*
539 *Evolution* **18**, 563–569 (2001).

540 15. Willett, C. S. & Burton, R. S. Evolution of Interacting Proteins in the Mitochondrial
541 Electron Transport System in a Marine Copepod. *Mol Biol Evol* **21**, 443–453 (2004).
542 16. Bazin, E., Glémin, S. & Galtier, N. Population Size Does Not Influence Mitochondrial
543 Genetic Diversity in Animals. *Science* **312**, 570–572 (2006).
544 17. James, J. E., Piganeau, G. & Eyre-Walker, A. The rate of adaptive evolution in animal
545 mitochondria. *Molecular Ecology* **25**, 67–78 (2016).
546 18. Barreto, F. S. *et al.* Genomic signatures of mitonuclear coevolution across populations of
547 Tigriopus californicus. *Nature Ecology & Evolution* **2**, 1250–1257 (2018).
548 19. Hood, W. R. *et al.* The Mitochondrial Contribution to Animal Performance, Adaptation,
549 and Life-History Variation. *Integrative and Comparative Biology* **58**, 480–485 (2018).
550 20. Wolstenholme, D. R. Animal Mitochondrial DNA: Structure and Evolution. in
551 *International Review of Cytology* (eds. Wolstenholme, D. R. & Jeon, K. W.) vol. 141 173–216
552 (Academic Press, 1992).
553 21. Frank, S. A. & Hurst, L. D. Mitochondria and male disease. *Nature* **383**, 224–224 (1996).
554 22. Smith, S. R. T. & Connallon, T. The contribution of the mitochondrial genome to sex-
555 specific fitness variance. *Evolution* **71**, 1417–1424 (2017).
556 23. Gemmell, N. J., Metcalf, V. J. & Allendorf, F. W. Mother's curse: the effect of mtDNA on
557 individual fitness and population viability. *Trends in Ecology & Evolution* **19**, 238–244 (2004).
558 24. Cardullo, R. A. & Baltz, J. M. Metabolic regulation in mammalian sperm: Mitochondrial
559 volume determines sperm length and flagellar beat frequency. *Cell Motility* **19**, 180–188
560 (1991).

561 25. Holyoake, A. J. *et al.* High incidence of single nucleotide substitutions in the
562 mitochondrial genome is associated with poor semen parameters in men. *International*
563 *Journal of Andrology* **24**, 175–182 (2001).
564 26. M. Florencia Camus, David J. Clancy, & Damian K. Dowling. Mitochondria, Maternal
565 Inheritance, and Male Aging. *Current Biology* **22**, 1717–1721 (2012).
566 27. Wade, M. J. & Brandvain, Y. REVERSING MOTHER'S CURSE: SELECTION ON MALE
567 MITOCHONDRIAL FITNESS EFFECTS. *Evolution* **63**, 1084–1089 (2009).
568 28. Unckless, R. L. & Herren, J. K. Population genetics of sexually antagonistic mitochondrial
569 mutants under inbreeding. *Journal of Theoretical Biology* **260**, 132–136 (2009).
570 29. Hedrick, P. W. REVERSING MOTHER'S CURSE REVISITED. *Evolution* **66**, 612–616 (2012).
571 30. Innocenti, P., Morrow, E. H. & Dowling, D. K. Experimental Evidence Supports a Sex-
572 Specific Selective Sieve in Mitochondrial Genome Evolution. *Science* **332**, (2011).
573 31. Camus, M. F., Wolf, J. B. W., Morrow, E. H. & Dowling, D. K. Single Nucleotides in the
574 mtDNA Sequence Modify Mitochondrial Molecular Function and Are Associated with Sex-
575 Specific Effects on Fertility and Aging. *Curr Biol* **25**, 2717–2722 (2015).
576 32. Camus, M. F. & Dowling, D. K. Mitochondrial genetic effects on reproductive success:
577 signatures of positive intrasexual, but negative intersexual pleiotropy. 10.
578 33. Wolff, J. N. *et al.* Evolutionary implications of mitochondrial genetic variation:
579 mitochondrial genetic effects on OXPHOS respiration and mitochondrial quantity change
580 with age and sex in fruit flies. *Journal of Evolutionary Biology* **29**, 736–747 (2016).
581 34. Carnegie, L., Reuter, M., Fowler, K., Lane, N. & Camus, M. F. Mother's curse is pervasive
582 across a large mitonuclear Drosophila panel. *Evolution Letters* **5**, 230–239 (2021).

583 35. Mossman, J. A., Tross, J. G., Li, N., Wu, Z. & Rand, D. M. Mitochondrial-Nuclear
584 Interactions Mediate Sex-Specific Transcriptional Profiles in Drosophila. *Genetics* **204**, 613–
585 630 (2016).
586 36. Mossman, J. A., Biancani, L. M. & Rand, D. M. Mitonuclear Epistasis for Development
587 Time and its Modification by Diet in Drosophila. *Genetics* (2016)
588 doi:10.1534/genetics.116.187286.
589 37. Immonen, E., Collet, M., Goenaga, J. & Arnqvist, G. Direct and indirect genetic effects of
590 sex-specific mitonuclear epistasis on reproductive ageing. *Heredity* **116**, 338–339 (2016).
591 38. Đorđević, M. *et al.* Sex-specific mitonuclear epistasis and the evolution of mitochondrial
592 bioenergetics, ageing, and life history in seed beetles: SEX-SPECIFIC MITONUCLEAR
593 EPISTASIS. *Evolution* **71**, 274–288 (2017).
594 39. Ashburner, M., Golic, K. G., Hawley, R. S., & others. *Drosophila: a laboratory handbook.*
595 (Cold spring harbor laboratory press, 2004).
596 40. Lane, N. The Costs of Breathing. *Science* **334**, 184–185 (2011).
597 41. Burton, R. S., Feldman, M. W. & Curtsinger, J. W. Population genetics of Tigriopus
598 californicus (Copepoda: Harpacticoida): I. Population structure along the central California
599 coast. *Marine Ecology Progress Series* 29–39 (1979).
600 42. Burton, R. S. Intraspecific Phylogeography Across the Point Conception Biogeographic
601 Boundary. *Evolution* **52**, 734–745 (1998).
602 43. Edmands, S. Phylogeography of the intertidal copepod Tigriopus californicus reveals
603 substantially reduced population differentiation at northern latitudes. *Molecular Ecology* **10**,
604 1743–1750 (2001).

605 44. Edmands, S. Heterosis and Outbreeding Depression in Interpopulation Crosses Spanning
606 a Wide Range of Divergence. *Evolution* **53**, 1757–1768 (1999).
607 45. Pritchard, V. L. & Edmands, S. THE GENOMIC TRAJECTORY OF HYBRID SWARMS:
608 OUTCOMES OF REPEATED CROSSES BETWEEN POPULATIONS OF *TIGRIOPUS CALIFORNICUS*:
609 *TIGRIOPUS CALIFORNICUS* HYBRID SWARMS. *Evolution* **67**, 774–791 (2013).
610 46. Voordouw, M. J. & Anholt, B. R. Heritability of sex tendency in a harpacticoid copepod,
611 Tigriopus californicus. *Evolution* **56**, 1754–1763 (2002).
612 47. Foley, B. R., Rose, C. G., Rundle, D. E., Leong, W. & Edmands, S. Postzygotic isolation
613 involves strong mitochondrial and sex-specific effects in Tigriopus californicus, a species
614 lacking heteromorphic sex chromosomes. *Heredity* **111**, 391–401 (2013).
615 48. Alexander, H. J., Richardson, J. M. L., Edmands, S. & Anholt, B. R. Sex without sex
616 chromosomes: genetic architecture of multiple loci independently segregating to determine
617 sex ratios in the copepod *Tigriopus californicus*. *Journal of Evolutionary Biology* **28**, 2196–
618 2207 (2015).
619 49. Willett, C. S. Potential Fitness Trade-Offs for Thermal Tolerance in the Intertidal
620 Copepod Tigriopus Californicus. *Evolution* **64**, 2521–2534 (2010).
621 50. Kelly, M. W., Sanford, E. & Grosberg, R. K. Limited potential for adaptation to climate
622 change in a broadly distributed marine crustacean. *Proc Biol Sci* **279**, 349–356 (2012).
623 51. Leong, W., Sun, P. Y. & Edmands, S. Latitudinal Clines in Temperature and Salinity
624 Tolerance in Tidepool Copepods. *Journal of Heredity* **109**, 71–77 (2018).
625 52. Foley, H. B. *et al.* Sex-specific stress tolerance, proteolysis, and lifespan in the
626 invertebrate Tigriopus californicus. *Experimental Gerontology* **119**, 146–156 (2019).

627 53. Bartoń, K. *MuMIn: Multi-Model Inference*. (2020).

628 54. Lenth, R. V. *emmeans: Estimated Marginal Means, aka Least-Squares Means*. (2020).

629 55. Bates, D., Mächler, M., Bolker, B. & Walker, S. Fitting Linear Mixed-Effects Models Using

630 lme4. *Journal of Statistical Software* **67**, 1–48 (2015).

631 56. Fox, J. & Weisberg, S. *An R Companion to Applied Regression*. (Sage, 2019).

632 57. Gompertz, B. On the Nature of the Function Expressive of the Law of Human Mortality,

633 and on a New Mode of Determining the Value of Life Contingencies. (1815)

634 doi:10.1098/rspl.1815.0271.

635 58. Jackson, C. flexsurv: A Platform for Parametric Survival Modeling in R. *Journal of*

636 *Statistical Software* **70**, 1–33 (2016).

637 59. R Core Team. *R: A Language and Environment for Statistical Computing*. (R Foundation

638 for Statistical Computing, 2020).

639 60. Canty, A. & Ripley, B. D. *boot: Bootstrap R (S-Plus) Functions*. (2020).

640 61. Davison, A. C. & Hinkley, D. V. *Bootstrap Methods and Their Applications*. (Cambridge

641 University Press, 1997).

642 62. Arnholt, A. T. & Evans, B. *BSDA: Basic Statistics and Data Analysis*. (2017).

643 63. Bolger, A. M., Lohse, M. & Usadel, B. Trimmomatic: a flexible trimmer for Illumina

644 sequence data. *Bioinformatics* **30**, 2114–2120 (2014).

645 64. Dierckxsens, N., Mardulyn, P. & Smits, G. NOVOPlasty: de novo assembly of organelle

646 genomes from whole genome data. *Nucleic Acids Research* **45**, e18 (2017).

647 65. Bernt, M. *et al.* MITOS: Improved de novo metazoan mitochondrial genome annotation.

648 *Molecular Phylogenetics and Evolution* **69**, 313–319 (2013).

649 66. Lunter, G. & Goodson, M. Stampy: A statistical algorithm for sensitive and fast mapping
650 of Illumina sequence reads. *Genome Res.* **21**, 936–939 (2011).
651 67. Picard Tools - By Broad Institute. https://broadinstitute.github.io/picard/.
652 68. Li, H. A statistical framework for SNP calling, mutation discovery, association mapping
653 and population genetical parameter estimation from sequencing data. *Bioinformatics* **27**,
654 2987–2993 (2011).
655 69. Darling, A. E., Mau, B. & Perna, N. T. progressiveMauve: Multiple Genome Alignment
656 with Gene Gain, Loss and Rearrangement. *PLoS ONE* **5**, e11147 (2010).
657 70. Ranwez, V., Douzery, E. J. P., Cambon, C., Chantret, N. & Delsuc, F. MACSE v2: Toolkit for
658 the Alignment of Coding Sequences Accounting for Frameshifts and Stop Codons. *Mol Biol*
659 *Evol* **35**, 2582–2584 (2018).
660 71. Larkin, M. A. *et al.* Clustal W and Clustal X version 2.0. *Bioinformatics* **23**, 2947–2948
661 (2007).
662 72. Yang, Z. PAML 4: Phylogenetic Analysis by Maximum Likelihood. *Mol Biol Evol* **24**, 1586–
663 1591 (2007).
664 73. Kofler, R. *et al.* PoPoolation: A Toolbox for Population Genetic Analysis of Next
665 Generation Sequencing Data from Pooled Individuals. *PLoS ONE* **6**, (2011).
666 74. Dowling, D. K. & Adrian, R. E. Challenges and Prospects for Testing the Mother's Curse
667 Hypothesis. *Integrative and Comparative Biology* **59**, 875–889 (2019).
668 75. Zhang, H., Guillaume, F. & Engelstädter, J. THE DYNAMICS OF MITOCHONDRIAL
669 MUTATIONS CAUSING MALE INFERTILITY IN SPATIALLY STRUCTURED POPULATIONS:

670 MITOCHONDRIA, MALE INFERTILITY & SPATIAL STRUCTURE. *Evolution* **66**, 3179–3188
671 (2012).
672 76. Vittor, B. A. Effects of the environment of fitness-related life history characters in
673 Tigriopus californicus. (University of Oregon, 1971).
674 77. Burton, R. S. Mating system of the intertidal copepod Tigriopus californicus. *Marine*
675 *Biology* **86**, 247–252 (1985).
676 78. Singh, S. R., Singh, B. N. & Hoenigsberg, H. F. Female remating, sperm competition and
677 sexual selection in Drosophila. *Genet Mol Res* **1**, 178–215 (2002).
678 79. Palmer, C. A. & Edmands, S. Mate choice in the face of both inbreeding and outbreeding
679 depression in the intertidal copepod Tigriopus californicus. *Marine Biology* **136**, 693–698
680 (2000).
681 80. Burton, R. S. Genetic Evidence for Long Term Persistence of Marine Invertebrate
682 Populations in an Ephemeral Environment. *Evolution* **51**, 993 (1997).
683 81. Dybdahl, M. F. Extinction, recolonization, and the genetic structure of tidepool copepod
684 populations. *Evol Ecol* **8**, 113–124 (1994).
685 82. Orr, H. A. Genetics of sterility in hybrids between two subspecies of Drosophila.
686 *Evolution* **43**, 180–189 (1989).
687 83. Turelli, M. & Orr, H. A. Dominance, Epistasis, and the Genetics of Postzygotic Isolation.
688 *Genetics* **154**, 1663–1679 (2000).
689 84. Pichaud, N., Ballard, J. W. O., Tanguay, R. M. & Blier, P. U. Mitochondrial haplotype
690 divergences affect specific temperature sensitivity of mitochondrial respiration. *J Bioenerg*
691 *Biomembr* **45**, 25–35 (2013).

692 85. Strehler, B. L. & Mildvan, A. S. General theory of mortality and aging. *Science* **132**, 14–21
693 (1960).
694 86. Li, N., Arief, N. & Edmands, S. Effects of oxidative stress on sex-specific gene expression
695 in the copepod Tigriopus californicus revealed by single individual RNA-seq. *Comparative*
696 *Biochemistry and Physiology Part D: Genomics and Proteomics* **31**, 100608 (2019).
697 87. Li, N., Flanagan, B. A., Partridge, M., Huang, E. J. & Edmands, S. Sex differences in early
698 transcriptomic responses to oxidative stress in the copepod Tigriopus californicus. *BMC*
699 *Genomics* **21**, 759 (2020).
700
701

702 SUPPLEMENTAL INFORMATION

703 Supplemental Information includes one document, three figures, and six tables and can be
704 found with this article online at xxx.
705

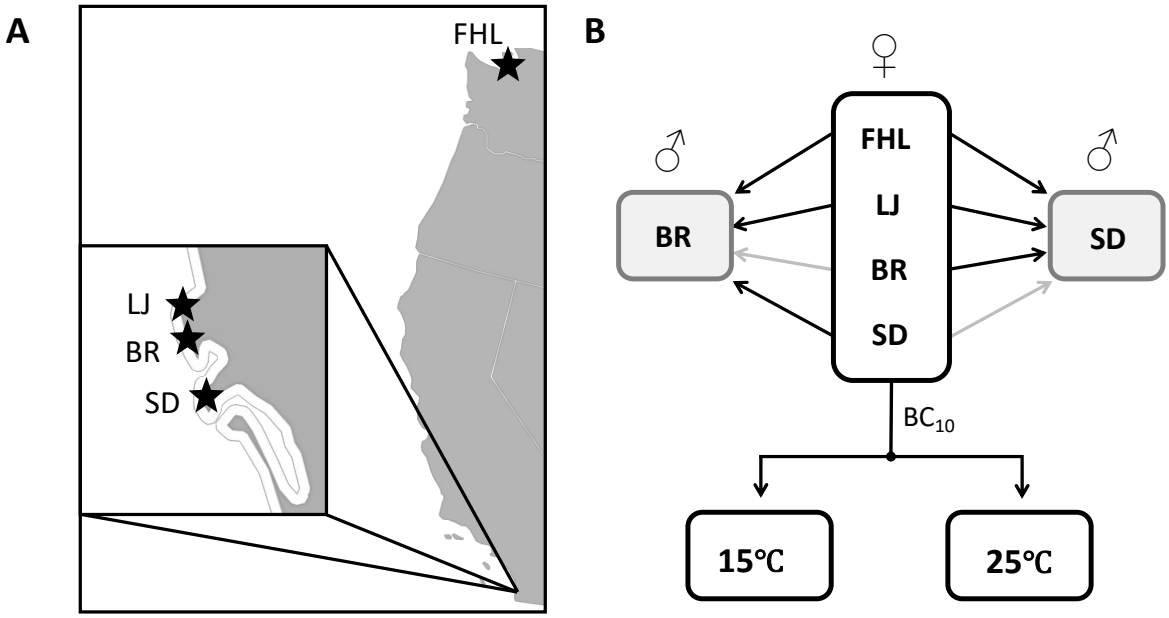

C

Backcross	Dam line	Sire line	Nuclear F_{ST}	mtDNA D_{XY}	mtDNA d_N	mtDNA d_S	% Paternal nDNA	% Maternal mtDNA	% Paternal mtDNA
SDxSD	SD	SD	0	0	0	0	100.00	94.09	94.09
BRxSD	BR	SD	0.102	0.096	0.023	0.532	99.90	97.22	0.28
LJxSD	LJ	SD	0.108	0.096	0.023	0.523	99.97	97.63	0.15
FHLxSD	FHL	SD	0.378	0.206	0.085	2.675	99.70	99.65	0.13
BRxBR	BR	BR	0	0	0	0	100.00	96.91	96.91
LJxBR	LJ	BR	0.049	0.007	0.002	0.046	99.93	95.96	0.08
SDxBR	SD	BR	0.102	0.096	0.023	0.532	99.72	95.32	0.02
FHLxBR	FHL	BR	0.369	0.211	0.085	4.347	99.15	99.81	0.02

Figure 1. Construction of mitonuclear hybrid panel

(A) Geographic location of populations used in this study – SD (San Diego, CA), BR (Bird Rock, CA), LJ (La Jolla, CA), FHL (Friday Harbor, WA). (B) Experimental design. Dams from the central panel were backcrossed to sires from BR and SD for 10 generations. Grey arrows indicate experimental control lines. Individuals from each line were reared at two contrasting temperatures, 15°C and 25°C. (C) DNA sequencing results from pool-seq. Measures of divergence (F_{ST}, D_{XY}, d_N, and d_S) were calculated between dam and sire line. Percent paternal nDNA and percent maternal/paternal mtDNA indicate minimal contaminating nDNA remaining in backcrossed individuals and the absence of paternal leakage of mtDNA.

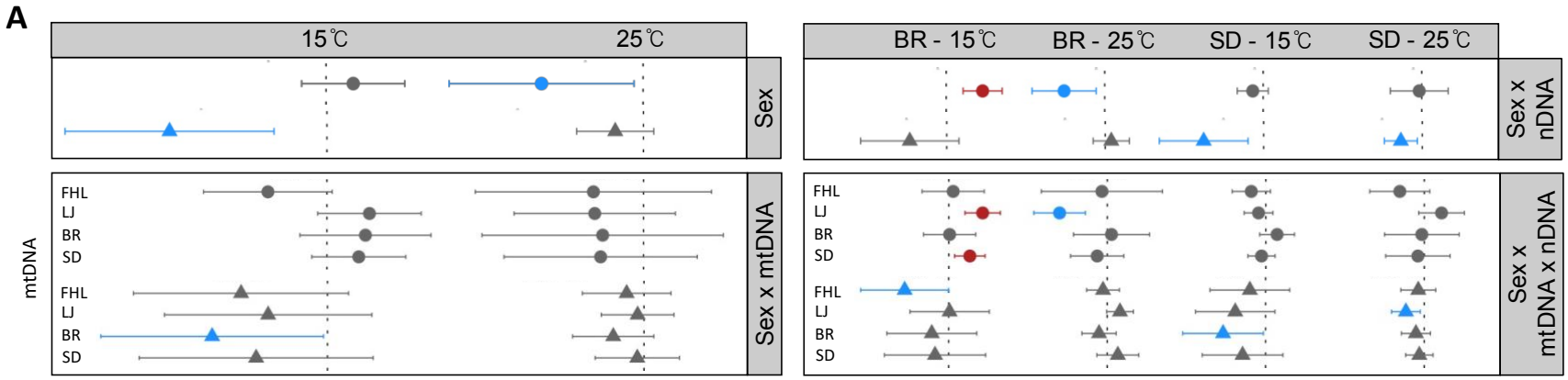

B

Trait	Temp.	nDNA	mtDNA	Sex	mtDNA x nDNA	Sex x mtDNA	Sex x nDNA	Sex x mtDNA x nDNA
Fertility	15℃	***	*	**	-	-	**	-
	25℃	NS	NS	NS	NS	NS	NS	*
Longevity	15℃	NS	NS	NS	NS	NS	NS	NS
	25℃	*	NS	NS	*	NS	NS	NS

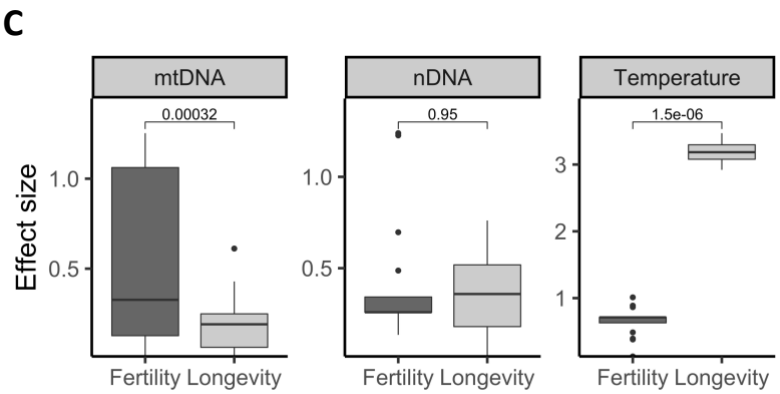

Figure 2. Trait modeling results.

(A) Model contrasts between the sexes were plotted for each sex-effect model (Sex, Sex x mtDNA, Sex x nDNA, and Sex x mtDNA x nDNA). Fertility contrasts are represented as circles and longevity contrasts as triangles. Points to the left of the dotted zero-line

indicate a higher mean in males and those to the right of the line indicate higher mean in females. Significant contrasts were colored to indicate the sex with the higher mean - red (higher female) or blue (higher male).

(B) Sex-effect model type III ANOVA table. Each row represents a separate model, with columns representing modeled fixed effects. Cells are marked with a dash when a variable is not included in the model. Abbreviations: NS – non significant ($p < 0.05$), ∗ – $p \leq 0.05$, ∗∗ – $p \leq 0.01$, ∗∗∗– $p \leq 0.001$.

(C) Genetic and temperature effect size comparisons between fitness traits. We estimated Cohen's *d* for all pairwise contrasts among temperature, mtDNA, and nDNA groupings. Contrasts were made on best fit linear mixed effects models for each sex and trait grouping (sex-specific fertility, longevity). Significance was determined using two-sample unpaired Wilcoxon rank sum tests with a two-sided alternate hypothesis and 95% confidence intervals. Sample sizes for contrasts were mtDNA, n = 96; nDNA, n = 32; and Temperature, n = 32.

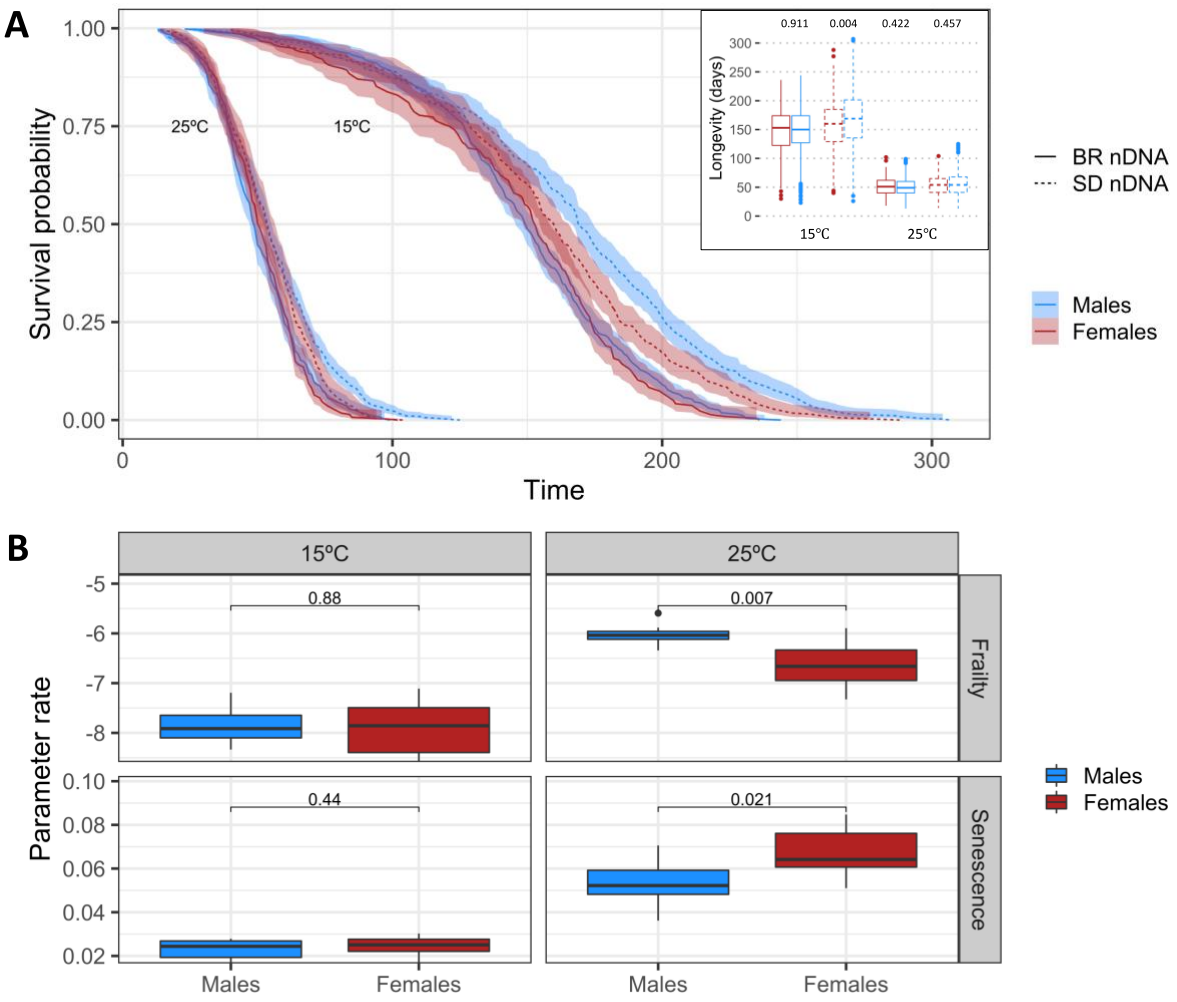

Figure 3. Males outlive females and have lower rates of senescence and higher frailty.

(A) Sex-specific survivorship curves based on nDNA and temperature groupings. Median longevity shown in insert with p-values indicating results of two-sample unpaired Wilcoxon rank sum tests with a two-sided alternate hypothesis and 95% confidence intervals.

(B) Sex contrasts for Gompertz parameters. We performed Wilcoxon tests as above to identify parametric differences in the rate of aging between the sexes.

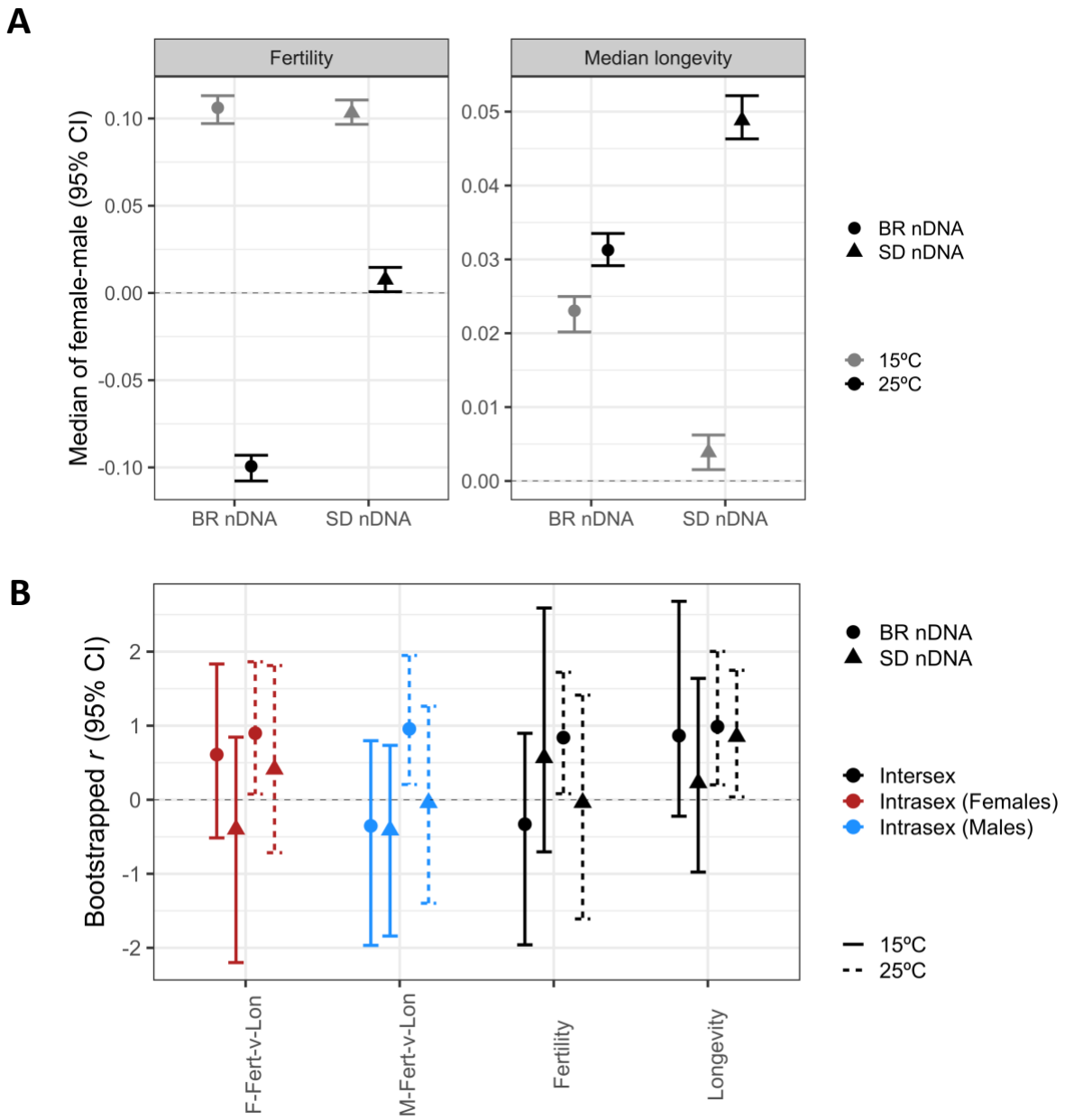

Figure 4. Testing the mother's curse hypothesis with mitonuclear hybrid *T. californicus.*

(A) Sex differences in mitochondrial coefficient of variation (CV_{mt}) for fertility and longevity. We estimated CV_{mt} for both fertility and median longevity by temperature and nuclear line and performed a two-sided sign test on bootstrapped estimates (1000 samples). The sign test compares the difference between female and male median values with negative values indicating higher male CV_{mt}, while positive values indicate that females have higher $CV_{mt.}$. The

majority of groupings indicate higher mitochondrial genetic variation in females in contradiction to the mother's curse hypothesis. Only fertility in BR nDNA individuals reared at 15°C had significantly higher mitochondrial genetic variation in males.

(B) Intra- and intersexual genetic correlation for female and male fertility and longevity across mitochondrial haplotypes. Bootstrapped Pearson's correlation coefficients (95% confidence intervals) were plotted for both rearing temperatures (15℃: solid lines, 25℃: dotted lines). Abbreviations: F (females), M (males), fertility (females: hatching number, males: remating success), longevity (mean longevity). All significant intersexual correlations indicate positive values, suggesting the absence of sexually antagonistic pleiotropy predicted by the mother's curse hypothesis.